


^{18}F -Labeled Pyrido[3,4-*d*]pyrimidine as an Effective Probe for Imaging of L858R Mutant Epidermal Growth Factor Receptor

Hiroyuki Kimura,^{*,†,‡,#} Haruka Okuda,^{†,#} Masumi Ishiguro,[§] Kenji Arimitsu,^{‡,§} Akira Makino,^{||} Ryuichi Nishii,[⊥] Anna Miyazaki,[†] Yusuke Yagi,[†] Hiroyuki Watanabe,[†] Ikuo Kawasaki,[§] Masahiro Ono,[†] and Hideo Saji,^{*,†} 

[†]Graduate School of Pharmaceutical Sciences, Kyoto University, Kyoto 606-8501, Japan

[‡]Department of Analytical and Bioinorganic Chemistry, Kyoto Pharmaceutical University, Kyoto 607-8414, Japan

[§]School of Pharmacy and Pharmaceutical Sciences, Mukogawa Women's University, Hyogo 663-8179, Japan

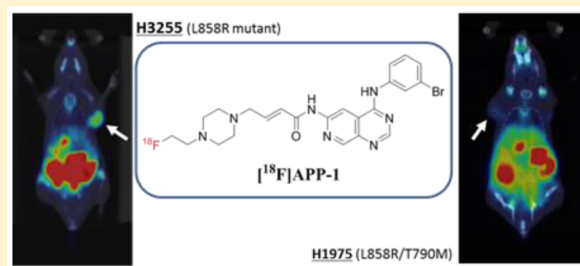
^{||}Biomedical Imaging Research Center (BIRC), University of Fukui, Fukui 910-1193, Japan

[⊥]National Institute of Radiological Sciences, Chiba 263-8555, Japan

Supporting Information

ABSTRACT: In nonsmall-cell lung carcinoma patients, L858R mutation of epidermal growth factor receptor (EGFR) is often found, and molecular target therapy using EGFR tyrosine kinase inhibitors is effective for the patients. However, the treatment frequently develops drug resistance by secondary mutation, of which approximately 50% is T790M mutation. Therefore, the ability to predict whether EGFR will undergo secondary mutation is extremely important. We synthesized a novel radiofluorinated 4-(anilino)pyrido[3,4-*d*]pyrimidine derivative (^{18}F]APP-1) and evaluated its potential as a positron emission tomography (PET) imaging probe to discriminate the difference in mutations of tumors. EGFR inhibition assay, cell uptake, and biodistribution study showed that ^{18}F]APP-1 binds specifically to the L858R mutant EGFR but not to the L858R/T790M mutant. Finally, on PET imaging study using ^{18}F]APP-1 with tumor-bearing mice, the H3255 tumor (L858R mutant) was more clearly visualized than the H1975 tumor (L858R/T790M mutant).

KEYWORDS: Epidermal growth factor receptor tyrosine kinase (EGFR-TK), L858R mutant EGFR, positron emission tomography, fluorin-18, 4-(anilino)pyrido[3,4-*d*]pyrimidine



Nonsmall-cell lung carcinoma (NSCLC) is a class of lung cancer that accounts for 80% of lung cancer cases and is a major cause of cancer-related deaths. In approximately 10–30% of patients with NSCLC, a somatic activating mutation occurs in the tyrosine kinase (TK) domain of the epidermal growth factor receptor (EGFR) and causes the exon 21 mutation, resulting in leucine being replaced by arginine at position 858 (L858R mutant) or exon 19 deletions in the EGFR gene.¹ The increased kinase activity of mutant EGFR plays a key role in cell proliferation and angiogenesis in cancer cells. Therefore, EGFR-TK inhibitors (EGFR-TKIs), such as gefitinib (Iressa), erlotinib (Tarceva), and afatinib (Giotrif), are used in NSCLC therapy to bind to the ATP domain in mutant EGFR-TK.²

However, patients who initially respond to EGFR-TKIs typically develop drug resistance within 6–12 months after the start of therapy, thereby inevitably disrupting the therapy.³ The most common factor is the occurrence of secondary mutation of the mutant EGFR gene, which leads to methionine replacing threonine at position 790 of EGFR (T790M mutation). The T790M mutation occurs in approximately 50% of patients with resistance to EGFR-TKIs.^{3,4} Therefore, predicting whether EGFR undergoes this secondary mutation is extremely

important for planning the treatment of EGFR-TKIs. For clinical settings, genetic testing is conducted via biopsy to find mutations and provide a definitive cancer diagnosis before starting the therapy.⁵ However, because of the invasiveness of this procedure, such testing is done only when the effect of molecular targeting drugs decreases over the course of treatment. Therefore, developing noninvasive diagnostics techniques that can determine the therapeutic efficiency of EGFR-TKIs has become necessary.

Positron emission tomography (PET) is a molecular imaging technique that enables noninvasive detection of specific molecules in living systems and is expected, in particular, to detect the presence of mutant EGFR. Furthermore, some radiolabeled EGFR-TKIs, including ^{18}F]gefitinib, ^{18}F]afatinib, and ^{11}C]erlotinib, have been investigated using PET probes for EGFR-TK-positive tumor imaging.^{6–12} However, the use of these compounds does not permit visualization of an EGFR-

Received: December 28, 2016

Accepted: March 20, 2017

Published: March 20, 2017

TK-positive tumor. In addition, the use of [^{11}C]erlotinib reportedly allows primary and secondary mutant tumors to be differentiated by visualizing the former but not the latter,¹² and it leads to unclear images of L858R mutant tumors, similar to the results for other radiolabeled EGFR-TKIs.

Previous investigations of a series of 4-(anilino)pyrido[3,4-*d*]pyrimidine derivatives as EGFR-TKIs claim that these compounds show lower half-maximal inhibitory concentration (IC_{50}) to EGFR-TK compared with 4-(anilino)quinazoline.^{13–15} Therefore, the radiolabeled 4-(anilino)pyrido[3,4-*d*]pyrimidine derivative is also expected to become an imaging-probe candidate for tumors targeted by EGFR-TKIs. In addition, we aimed drug design on the grounds that incorporating a Michael acceptor unit at position 6 of pyrido[3,4-*d*]pyrimidine and quinazoline scaffolds leads to irreversible inhibition of EGFR-TK through a covalent modification of cysteine 797 in the ATP binding domain^{16–18} and that the piperazinyl group is useful to afford suitable water solubility and induce the radiolabeling site. Moreover, if the accumulation of the derivative differs between the primary and secondary mutant tumor, we hope to use 4-(anilino)pyrido[3,4-*d*]pyrimidine as an imaging probe to identify whether EGFR mutations are present. In the present study, we synthesize a novel radiofluorinated 4-(anilino)pyrido[3,4-*d*]pyrimidine derivative APP-1 (Figure 1) and evaluate its ability to discriminate between primary and secondary mutations in *in vitro* and *in vivo* experiments.

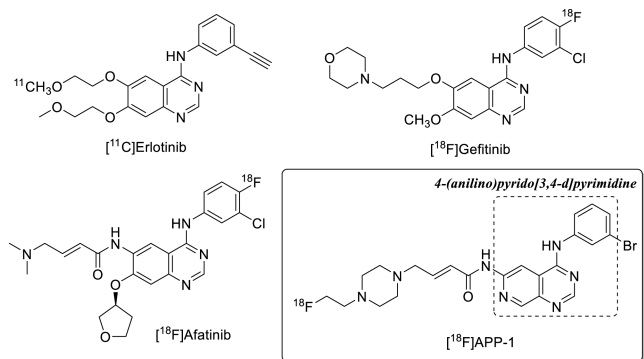


Figure 1. Chemical structure of EGFR-targeting PET imaging probes.

The nonradioactive APP-1 was synthesized as indicated in Scheme 1. First, 6-aminopyrido[3,4-*d*]pyrimidine 1 was

prepared from 2-fluoro-5-aminopyridine via the synthetic route reported by Newcastle et al.¹⁴ Compound 1 was coupled with 4-bromocrotonic acid by using 1-(3-(dimethylamino)propyl)-3-ethylcarbodiimide hydrochloride as the condensing agent followed by the addition of 1-(*tert*-butyloxycarbonyl)piperazine to obtain amide 2 at a 91% yield. The deprotection of the *tert*-butyloxycarbonyl group of compound 2 gave amine 3. Finally, compound 3 was reacted with 2-fluoroethyl tosylate to obtain APP-1.

The inhibition assay of APP-1 involved using erlotinib and AZD9291 to inhibit the L858R mutant and L858R/T790M mutant EGFR-TK; the results for IC_{50} appear in Table 1.

Table 1. IC_{50} for APP-1, Erlotinib, and AZD9291

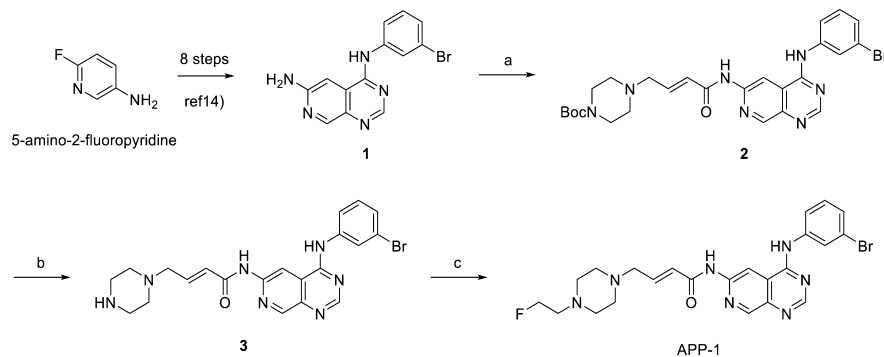
compd	IC_{50}^a (nM)	
	L858R	L858R/T790M
APP-1	15.6 ± 0.8	326 ± 64
Erlotinib	12.5 ± 6.0	4040 ± 1270
AZD9291	12.3 ± 3.1	14.5 ± 5.3

^aThe values represent the mean ± SE ($n = 3$).

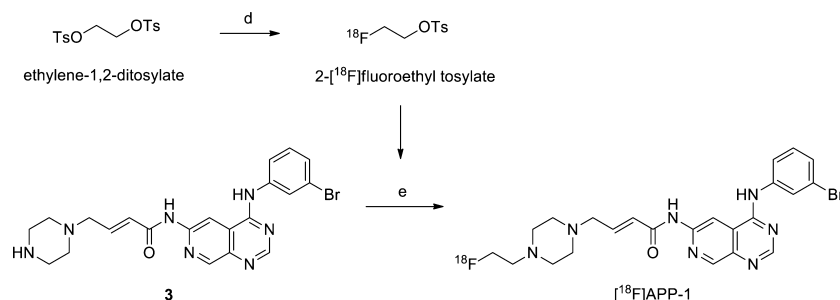
Erlotinib inhibits the L858R mutant EGFR kinase but not the L858R/T790M mutant,¹² and AZD9291 (osimertinib, Targrisso), developed by AstraZeneca to inhibit the L858R/T790M mutant EGFR-TK and recently approved by the US Food and Drug Administration, inhibits both the L858R and L858R/T790M mutants of EGFR-TK.¹⁹ As a result, both APP-1 and erlotinib inhibit L858R mutant EGFR-TK somewhat more than L858R/T790M mutant of EGFR-TK (15.6 ± 0.8 nM vs 326 ± 64 nM and 12.5 ± 6.0 nM vs 4040 ± 1270 nM, respectively), and AZD9291 potently inhibits mutant EGFR-TK (12.3 ± 3.1 nM vs 14.5 ± 5.3 nM). Thus, radioactive APP-1 is also expected to become a probe candidate for imaging EGFR-TK-positive tumors. In addition, APP-1 is found to be selective, although the range of selectivity is smaller than that of erlotinib. However, whether its selectivity suffices to visually discriminate between L858R- and L858R/T790M mutant tumors remains to be determined. Therefore, we continue evaluating the potential of APP-1 for use in PET imaging.

We synthesized ^{18}F -labeled [^{18}F]APP-1 from precursor 3 in a two-step reaction (Scheme 2). First, we prepared radioactive 2- [^{18}F]fluoroethyl tosylate by a nucleophilic displacement reaction of ethylene glycol-1,2-ditosylate with the [^{18}F]fluoride anion. After purification by preparative high-

Scheme 1. Synthesis of Nonradioactive APP-1 and Its Precursor 3^a



^aReagents and conditions: (a) 4-bromocrotonic acid, 1-(3-(dimethylamino)propyl)-3-ethylcarbodiimide hydrochloride, DIPEA, DMF, rt, 1 h followed by 1-(*tert*-butyloxycarbonyl)piperazine, rt, 30 min, 91%; (b) TFA, dichloromethane, rt, 85%; (c) 2-fluoroethyl tosylate, Et₃N, DMF, rt, 45%.

Scheme 2. Radiosynthesis of [^{18}F]APP-1^a

^aReagent and conditions: (d) potassium [^{18}F]fluoride, Kryptofix 2.2.2, MeCN, 90 °C, 5 min; and (e) Et₃N, DMF, 110 °C, 20 min, 3.2 ± 0.94% radiochemical yield ($n = 5$, EOS from potassium [^{18}F]fluoride).

performance liquid chromatography (HPLC) and solid-phase extraction, 2-[^{18}F]fluoroethyl tosylate was reacted with compound 3 for 20 min at 110 °C to yield [^{18}F]APP-1 in a radiochemical yield of 3.2 ± 0.94% [$n = 5$, end of synthesis (EOS), from potassium [^{18}F]fluoride] after preparative HPLC. The total operation took less than 110 min. The isolated [^{18}F]APP-1 was identified by a HPLC analysis with coinjection of APP-1 (Figure 2). The radiochemical purity and the specific activity exceeded 95% and 40.4 GBq/ μmol , respectively.

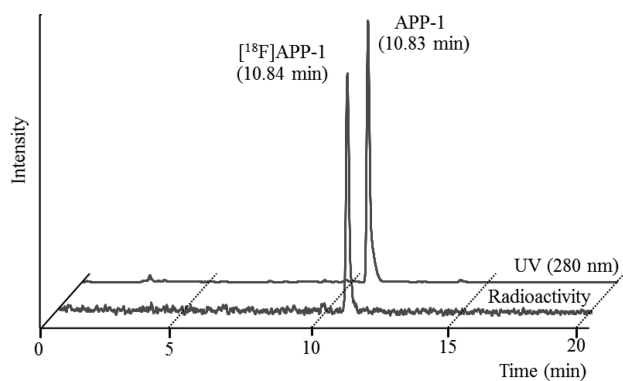


Figure 2. HPLC analysis of [^{18}F]APP-1 coinjected with nonradioactive APP-1. HPLC conditions: the column was a Cosmosil 5C₁₈-AR-II 10 mm × 250 mm; flow rate was 5.0 mL/min; UV excitation at 280 nm; and mobile phase systems were MeCN (0.1% TFA)/H₂O (0.1% TFA) = 20:80 (0 min) to 40:60 (20 min).

We next investigated the cellular uptake of [^{18}F]APP-1 by two human NSCLC cells: H3255 cells expressing the L858R mutant EGFR and H1975 cells expressing the L858R/T790M mutant. The results appear in Figure 3. The uptake of [^{18}F]APP-1 in H3255 cells was twice as much as that in the H1975 cells. Furthermore, upon adding AZD9291 as inhibitor, the H3255-cell uptake decreases (104% ± 8.6% dose/mg protein to 46.8% ± 7.6% dose/mg protein, $P < 0.01$), whereas the uptake of H1975 cells remains stable. This result suggests that the different uptake is caused by the specific binding of [^{18}F]APP-1 to L858R mutant EGFR-TK. Because the inhibition rate of H3255 did not change even when 5 μM or more of AZD9291 was added (data not shown), incomplete blockade of H3255 cells may represent nonspecific binding.

We studied the biodistribution of [^{18}F]APP-1 in H3255-tumor-bearing mice (Table 2). The highest accumulation of [^{18}F]APP-1 occurred in the intestines [small intestine, 44.94% injected dose per gram (ID/g) at 1 h postinjection; colon,

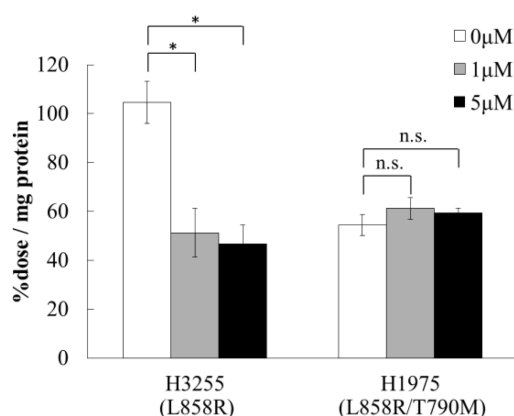


Figure 3. Accumulation of [^{18}F]APP-1 in H3255 and H1975 cells after incubation with and without AZD9291. The values represent the mean ± standard deviation ($n = 3$; * $P < 0.01$; “n.s.” means “not significant”).

Table 2. Biodistribution of [^{18}F]APP-1 in H3255-Tumor-Bearing Mice^a

tissue	Injected dose/g (%)	
	1 h after injection	3 h after injection
blood	1.60 ± 0.33	1.12 ± 0.08
heart	1.61 ± 0.38	0.72 ± 0.12
lung	3.48 ± 0.51	1.18 ± 0.14
stomach	17.93 ± 7.12	3.64 ± 1.68
small intestine	44.94 ± 5.51	14.70 ± 4.31
colon	6.96 ± 0.61	59.65 ± 11.68
liver	7.86 ± 1.23	2.78 ± 0.38
pancreas	5.80 ± 0.78	1.12 ± 0.12
spleen	4.37 ± 0.50	1.08 ± 0.17
kidney	8.58 ± 1.25	2.05 ± 0.22
bone	0.81 ± 0.46	1.32 ± 0.40
muscle	0.63 ± 0.21	0.29 ± 0.06
tumor (H3255)	3.62 ± 0.87	3.80 ± 0.88
ratios		
tumor/blood	2.25 ± 0.18	3.35 ± 0.66
tumor/muscle	6.15 ± 1.88	13.37 ± 4.02
tumor/lung	1.04 ± 0.20	3.21 ± 0.54

^aThe values represent the mean ± SD ($n = 5$).

59.65% ID/g at 3 h postinjection] and was excreted over time. The accumulation of [^{18}F]APP-1 in bone was low. Therefore, [^{18}F]APP-1 was stable *in vivo*. The accumulation of [^{18}F]APP-1 in tumors was retained for at least 3 h (3.62% ID/g at 1 h postinjection, 3.80% ID/g at 3 h postinjection). Because the

accumulation of [^{11}C]erlotinib for 1 h in H3255 tumors is reported to be decreasing over time,⁹ we assume that [^{18}F]APP-1 strongly binds to EGFR-TK in H3255 tumors by irreversible binding associated with a covalent bond via the Michael acceptor group. However, the slow clearance from normal tissue must be improved. At each time point, Table 2 also gives the tumor-to-blood, tumor-to-muscle, and tumor-to-lung ratios. All ratios increase over time and exceed three at 3 h postinjection. Therefore, we expect the use of [^{18}F]APP-1 for visualization of H3255 tumors in mice.

Furthermore, we studied *in vivo* blocking to determine the ability of [^{18}F] to discriminate between L858R and L858R/T790M mutant EGFRs (Figure 4). Coadministration of excess

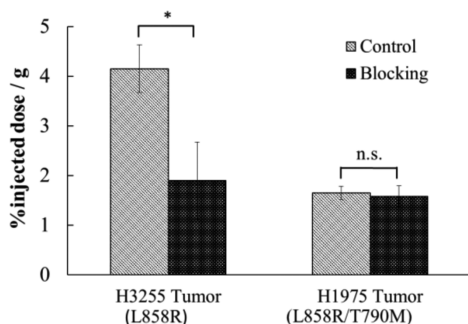


Figure 4. Effect of coadministration of AZD9291 on biodistribution of [^{18}F]APP-1 (3 h postinjection). The graphs show the mean %ID/g of four mice with the error bars giving the standard deviation (* $P < 0.01$).

AZD9291 significantly reduced the accumulation of [^{18}F]APP-1 in H3255 tumors (54% inhibition) at 3 h postinjection. However, accumulation in H1975 tumors was not blocked by excess AZD9291. These results correspond to those of the cell uptake study (Figure 3). In other words, these results confirm that, in mice with mutant-EGFR-TK tumors, [^{18}F]APP-1 binds specifically to L858R mutant EGFR-TK but not to L858R/T790M mutant EGFR-TK.

Furthermore, we performed PET imaging of [^{18}F]APP-1 in H3255- or H1975-tumor-bearing mice (Figure 5). The images at 3 h postinjection of [^{18}F]APP-1 show that H3255 tumors are more clearly visualized than H1975 tumors. In addition, we measured the radioactivity in each organ and tissue after image acquisition and calculated the tumor-to-blood, tumor-to-muscle, and tumor-to-lung ratios (Table 3). The contrast between H3255 tumors and surrounding tissue is higher than that when using [^{11}C]erlotinib.¹³ These results suggest that [^{18}F]APP-1 is effective as an imaging probe that targets L858R mutant EGFR.

We designed and synthesized a radiofluorinated 4-(anilino)-pyrido[3,4-*d*]pyrimidine derivative, APP-1, as a PET imaging agent to discriminate between L858R and L858R/T790M mutant EGFRs. When used in an EGFR-TK inhibition assay, APP-1 was the strongest inhibitor of the L858R mutant EGFR-TK, and a weak inhibitor of the L858R/T790M mutant EGFR-TK. The cell-uptake study shows that [^{18}F]APP-1 binds specifically to the L858R mutant EGFR-TK but not to the L858R/T790M mutant. Further assessment of the biodistribution revealed that [^{18}F]APP-1 results in a high tumor-to-tissue ratio in H3255-tumor-bearing mice, while coinjection of AZD9291 suggests that the accumulation of [^{18}F]APP-1 in tumors is specific to EGFR-TK. In addition, for PET imaging,

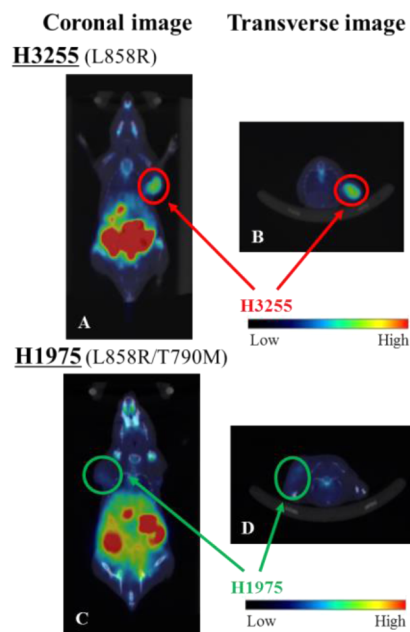


Figure 5. PET-CT image of [^{18}F]APP-1 (A,B) in H3255- or (C,D) in H1975-tumor-bearing mice at 3 h postinjection. Panels (A) and (C) show coronal images, while panels (B) and (D) show transverse images.

Table 3. Ratios of Accumulated Radioactivity in H3255 and H1975 Tumor-Bearing Mice after PET-CT Imaging

tumor	ratio		
	tumor/blood	tumor/muscle	tumor/lung
H3255	3.12	6.80	3.25
H1975	0.74	2.95	0.74

the H3255 tumor is more clearly visualized than the H1975 tumor. Based on these results, we conclude that [^{18}F]APP-1 has a potential to be used as a PET imaging probe to discriminate between L858R and L858R/T790M mutant EGFRs in NSCLC.

■ ASSOCIATED CONTENT

📄 Supporting Information

The Supporting Information is available free of charge on the ACS Publications website at DOI: 10.1021/acsmchemlett.6b00520.

Full experimental procedures and characterization data for all new compounds described in this study (PDF)

■ AUTHOR INFORMATION

Corresponding Authors

*E-mail: hkimura@mb.kyoto-phu.ac.jp.

*E-mail: hsaji@pharm.kyoto-u.ac.jp.

ORCID

Hideo Saji: 0000-0002-3077-9321

Author Contributions

#These authors have contributed equally. The manuscript was written through contributions of all authors, and all the authors approve the final version of the manuscript.

Funding

This work was supported by the Practical Research for Innovative Cancer Control from the Japan Agency for Medical

Research and Development (AMED) and Grants-in-Aid for Scientific Research from the Japan Society for the Promotion of Science.

Notes

The authors declare no competing financial interest.

ABBREVIATIONS

ATP, adenosine triphosphate; DIPEA, *N,N*-diisopropylethylamine; Boc, *tert*-butyloxycarbonyl; DMF, *N,N*-dimethylformamide; EGFR, epidermal growth factor receptor; EGFR-TK, epidermal growth factor receptor tyrosine kinase; EGFR-TKIs, epidermal growth factor receptor tyrosine kinase inhibitors; ID, injected dose; MeCN, acetonitrile; NSCLC, nonsmall-cell lung carcinoma; PET, positron emission tomography; HPLC, high-performance liquid chromatography; rt, room temperature; TFA, trifluoroacetic acid

REFERENCES

- (1) Janku, F.; Garrido-Laguna, I.; Petruzelka, L. B.; Stewart, D. J.; Kurzrock, R. Novel therapeutic targets in non-small cell lung cancer. *J. Thorac. Oncol.* **2011**, *6*, 1601–1612.
- (2) Ellis, P. M.; Coakley, N.; Feld, R.; Kuruvilla, S.; Ung, Y. C. Use of the epidermal growth factor receptor inhibitors gefitinib, erlotinib, afatinib, dacomitinib, and icotinib in the treatment of non-small-cell lung cancer: A systematic review. *Curr. Oncol.* **2015**, *22*, e183–e215.
- (3) Sharma, S. V.; Bell, D. W.; Settleman, J.; Haber, D. A. Epidermal growth factor receptor mutations in lung cancer. *Nat. Rev. Cancer* **2007**, *7*, 169–181.
- (4) Kobayashi, S.; Boggon, T. J.; Dayaram, T.; Jänne, P. A.; Kocher, O.; Meyerson, M.; Johnson, B. E.; Eck, M. J.; Tenen, D. G.; Halmos, B. EGFR mutation and resistance of non-small-cell lung cancer to gefitinib. *N. Engl. J. Med.* **2005**, *352*, 786–792.
- (5) Jackman, D.; Pao, W.; Riely, G. J.; Engelman, J. A.; Kris, M. G.; Jänne, P. A.; Lynch, T.; Johnson, B. E.; Miller, V. A. Clinical definition of acquired resistance to epidermal growth factor receptor tyrosine kinase inhibitors in non-small-cell lung cancer. *J. Clin. Oncol.* **2010**, *28*, 357–360.
- (6) Su, H.; Seimbille, Y.; Ferl, G. Z.; Bodenstern, C.; Fueger, B.; Kim, K. J.; Hsu, Y. T.; Dubinett, S. M.; Phelps, M. E.; Czernin, J.; Weber, W. A. Evaluation of [¹⁸F]gefitinib as a molecular imaging probe for the assessment of the epidermal growth factor receptor status in malignant tumors. *Eur. J. Nucl. Med. Mol. Imaging* **2008**, *35*, 1089–1099.
- (7) Slobbe, P.; Windhorst, A. D.; Walsum, M. S.; Schuit, R. C.; Smit, E. F.; Niessen, H. G.; Solca, F.; Stehle, G.; van Dongen, G. A. M. S.; Poot, A. J. Development of [¹⁸F]afatinib as new TKI-PET tracer for EGFR positive tumors. *Nucl. Med. Biol.* **2014**, *41*, 749–757.
- (8) Bonasera, T. A.; Ortu, G.; Rozena, Y.; Kraisa, R.; Freedman, N. M. T.; Chisina, R.; Gazit, A.; Levitzkib, A.; Mishani, E. Potential ¹⁸F-labeled biomarkers for epidermal growth factor receptor tyrosine kinase. *Nucl. Med. Biol.* **2001**, *28*, 359–374.
- (9) Dissoki, S.; Eshet, R.; Billauer, H.; Mishani, E. Modified PEG-anilinoquinazoline derivatives as potential EGFR PET agents. *J. Labelled Compd. Radiopharm.* **2009**, *52*, 41–52.
- (10) Memon, A. A.; Jakobsen, S.; Hansen, F. D.; Sorensen, B. S.; Keiding, S.; Nexø, E. Positron emission tomography (PET) imaging with [¹¹C]-labeled erlotinib: A micro-PET study on mice with lung tumor xenografts. *Cancer Res.* **2009**, *69*, 873–878.
- (11) Bahce, I.; Smit, E. F.; Lubberink, M.; van der Veldt, A. A. M.; Yaqub, M.; Windhorst, A. D.; Schuit, R. C.; Thunnissen, E.; Heideman, D. A. M.; Postmus, P. E.; Lammertsma, A. A.; Hendrikse, N. H. Development of [¹¹C]erlotinib positron emission tomography for *in vivo* evaluation of EGF receptor mutational status. *Clin. Cancer Res.* **2013**, *19*, 183–193.
- (12) Abourbeh, G.; Itamar, B.; Salnikov, O.; Beltsov, S.; Mishani, E. Identifying erlotinib-sensitive non-small cell lung carcinoma tumors in mice using [¹¹C]erlotinib PET. *EJNMMI Res.* **2015**, *5*, 4.
- (13) Bridges, A. J.; Zhou, H.; Cody, D. R.; Rewcastle, G. W.; McMichael, A.; Showalter, H. D. H.; Fry, D. W.; Kraker, A. J.; Denny, W. A. Tyrosine kinase inhibitors. 8. An unusually steep structure-activity relationship for analogues of 4-(3-bromoanilino)-6,7-dimethoxyquinazoline (PD 153035), a potent inhibitor of the epidermal growth factor receptor. *J. Med. Chem.* **1996**, *39*, 267–276.
- (14) Rewcastle, G. W.; Palmer, B. D.; Thompson, A. M.; Bridges, A. J.; Cody, D. R.; Zhou, H.; Fry, D. W.; McMichael, A.; Denny, W. A. Tyrosine kinase inhibitors. 10. isomeric 4-[(3-bromophenyl)amino]pyrido[*d*]pyrimidines are potent ATP binding site inhibitors of the tyrosine kinase function of the epidermal growth factor receptor. *J. Med. Chem.* **1996**, *39*, 1823–1835.
- (15) Rewcastle, G. W.; Murray, D. K.; Elliott, W. L.; Fry, D. W.; Howard, C. T.; Nelson, J. M.; Roberts, B. J.; Vincent, P. W.; Showalter, H. D. H.; Winters, R. T.; Denny, W. A. Tyrosine kinase inhibitors. 14. structure-activity relationships for methylamino-substituted derivatives of 4-[(3-bromophenyl)amino]-6-(methylamino)pyrido[3,4-*d*]pyrimidine (PD 158780), a potent and specific inhibitor of the tyrosine kinase activity of receptors for the EGF family of growth factors. *J. Med. Chem.* **1998**, *41*, 742–751.
- (16) Smaill, J. B.; Showalter, H. D. H.; Zhou, H.; Bridges, A. J.; McNamara, D. J.; Fry, D. W.; Nelson, J. M.; Sherwood, V.; Vincent, P. W.; Roberts, B. J.; Elliott, W. L.; Denny, W. A. Tyrosine kinase inhibitors. 18. 6-substituted 4-anilinoquinazolines and 4-anilinopyrido[3,4-*d*]pyrimidines as soluble, irreversible inhibitors of the epidermal growth factor receptor. *J. Med. Chem.* **2001**, *44*, 429–440.
- (17) Tsou, H. R.; Mamuya, N.; Johnson, B. D.; Reich, M. F.; Gruber, B. C.; Ye, F.; Nilakantan, R.; Shen, R.; Discifani, C.; DeBlanc, R.; Davis, R.; Koehn, F. E.; Greenberger, L. M.; Wang, Y. F.; Wissner, A. 6-Substituted-4-(3-bromophenylamino) quinazolines as putative irreversible inhibitors of the epidermal growth factor receptor (EGFR) and human epidermal growth factor receptor (HER-2) tyrosine kinases with enhanced antitumor activity. *J. Med. Chem.* **2001**, *44*, 2719–2734.
- (18) Klutchko, S. R.; Zhou, H.; Winters, R. T.; Tran, T. P.; Bridges, A. J.; Althaus, I. W.; Amato, D. M.; Elliott, W. L.; Ellis, P. A.; Meade, M. A.; Roberts, B. J.; Fry, D. W.; Gonzales, A. J.; Harvey, P. J.; Nelson, J. M.; Sherwood, V.; Han, H. K.; Pace, G.; Smaill, J. B.; Denny, W. A.; Showalter, H. D. H. Tyrosine kinase inhibitors. 19. 6-alkynamides of 4-anilinoquinazolines and 4-anilinopyrido[3,4-*d*]pyrimidines as irreversible inhibitors of the erbB family of tyrosine kinase receptors. *J. Med. Chem.* **2006**, *49*, 1475–1485.
- (19) Cross, D. A. E.; Ashton, S. E.; Ghiorghiu, S.; Eberlein, C.; Nebhan, C. A.; Spitzler, P. J.; Orme, J. P.; Finlay, M. R. V.; Ward, R. A.; Mellor, M. J.; Hughes, G.; Rahi, A.; Jacobs, V. N.; Brewer, M. R.; Ichihara, E.; Sun, J.; Jin, H.; Ballard, P.; Al-Kadhimi, K.; Rowlinson, R.; Klinowska, T.; Richmond, G. H. P.; Cantarini, M.; Kim, D. W.; Ranson, M. R.; Pao, W. AZD9291, an irreversible EGFR TKI, overcomes T790M-mediated resistance to EGFR inhibitors in lung cancer. *Cancer Discovery* **2014**, *4*, 1046–1061.